Technical University of Denmark

DTU

Numerical simulation of airfoil trailing edge serration noise

Zhu, Wei Jun; Shen, Wen Zhong

Link back to DTU Orbit

DTU Library
Technical Information Center of Denmark

Numerical simulation of airfoil trailing edge serration noise

**Wei Jun Zhu, Wen Zhong Shen
Technical University of Denmark, Lyngby 2800, DK.
E-mail: wjzh@dtu.dk**

Summary

In the present work, numerical simulations are carried out for a low noise airfoil with and without serrated Trailing Edge. The Ffowcs Williams-Hawkings acoustic analogy is implemented into the in-house incompressible flow solver EllipSys3D. The instantaneous hydrodynamic pressure and velocity field are obtained using Large Eddy Simulation. To obtain the time history data of sound pressure, the flow quantities are integrated around the airfoil surface through the FW-H approach. The extended length of the serration is about 16.7% of the airfoil chord and the geometric angle of the serration is 28 degrees. The chord based Reynolds number is around 1.5×10^6. Simulations are compared with existing wind tunnel experiments at various angles of attack. Even though the airfoil under investigation is already optimized for low noise emission, numerical simulations and wind tunnel experiments show that the noise level is further decreased by adding the TE serration device.

1. Introduction

As airfoil trailing edge (TE) noise is a main component of wind turbine aerodynamic noise, design of low noise wind turbine is directly related to low noise airfoil design. For existing wind turbine blades, it is possible to further decrease noise level by adding smart devices with active or passive flow controls at TE. Some large noise reduction was observed from previous wind tunnel and field experiments. As this major noise mechanism is well-known, smart design at TE using active or passive flow control become nature choices to decrease the total dB level. Active flow control, such as wall suction [1] has shown positive effect on the TE noise reduction by decreasing the boundary layer thickness at TE. Other active control, such as flow blowing flap [2], is demonstrated that the blowing greatly weakens the vortex system and decease noise generation. As a feasible technique, passive flow control methods for wind turbine blades seem practical. For example, the passive devices at TE can be either brushes [3, 4] and serrations [5,6,7,8,9]. The TE brushes and serrations for wind turbine applications are still under investigation. Physical understanding of flow mechanisms around serrations is needed in order to carry out detailed design work. Based on the assumption of a flat plate, Howe [6] derived a noise prediction model for a saw-tooth trailing edge at zero angle of attack. In his model, the far-field noise spectrum is related to the aerodynamic pressure spectrum. However, theoretical prediction using Howe's theory does not fit well with some of

the airfoil noise measurements [10]. It is expected that advanced computational aero-acoustic methods gives more accurate prediction of noise from a serrated trailing edge. Sandberg and Jones [11] performed direct numerical simulation (DNS) of a NACA 0012 airfoil. As the Reynolds number is low, the immersed boundary technique is applied to handle the complex saw-tooth geometry at TE. The study of Sandberg and Jones shows that TE noise is reduced at higher frequencies while no significant difference is seen at low frequencies. This might be related with specific Reynolds number and angle of attack. In the current work, the integrated representation of Ffowcs Williams-Hawkings (FW-H) acoustic analogy [12] is implemented into the in-house flow solver EllipSys3D. Simulations with and without TE serrations are performed at different angles of attack. Comparisons against measurements are performed for both flow and noise radiation. Results show relatively large noise reduction by introducing serration at airfoil trailing edge.

2. Numerical approach

In this work, the formulation 1 proposed by Farassat [13] is applied. The formulation is the solution of the FW-H equation with surface sources only when the surface moves at subsonic speed. This formulation has been successfully used for helicopter rotor and propeller noise predictions. At the retarded or emission time, the thickness and loading noise equations are written as

$$4\pi p'_T(\mathbf{x}, t) = \frac{\partial}{\partial t} \int_{f=0} \left[\frac{\rho_0 v_n}{r(1-M_r)} \right]_{ret} dS \tag{1}$$

$$4\pi p'_L(\mathbf{x}, t) = \frac{1}{c} \frac{\partial}{\partial t} \int_{f=0} \left[\frac{p \cos \theta}{r(1-M_r)} \right]_{ret} dS + \int_{f=0} \left[\frac{p \cos \theta}{r^2(1-M_r)} \right]_{ret} dS \tag{2}$$

The right hand sides of Eq. (1) and (2) are the integrations of time history variables obtained from flow calculations. The variables include wall normal velocity v_n, the Mach number of the source in the radiation direction M_r, the pressure on the solid wall surface p, the distance between source and receiver r, the angle between radiation direction and the local wall normal direction θ. Figure 1 shows a sketch of an airfoil where dS indicates one of the typical wall element that is integrated over the entire airfoil surface. It is obvious that the the angle θ will contribute to the noise directivity. The acoustic solver may run in parallel with flow model, in practice the acoustic solver starts when the flow-field is fully established. The necessary time history flow data are recoded in advance in order to calculate the time derivatives at emission time.
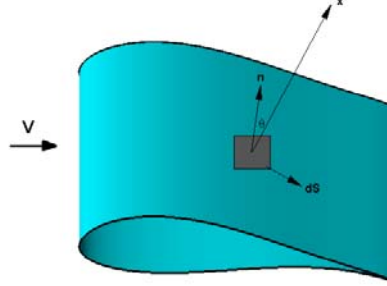
Figure 1. Sketch of the DTU-LN118 airfoil surface.

The filtered incompressible Navier-Stokes equations, momentum, turbulent stresses and eddy viscosity equations are applied to obtain the flow data.

$$\frac{\partial \overline{U}_i}{\partial t} + \frac{\partial (\overline{U}_i \overline{U}_j)}{\partial x_j} = -\frac{1}{\rho}\frac{\partial \overline{P}}{\partial x_i} + \nu \frac{\partial^2 \overline{U}_i}{\partial x_j^2} + \frac{\partial \tau_{ij}}{\partial x_j} \qquad (3)$$

$$\tau_{ij} = \nu_t \left(\frac{\partial \overline{U}_i}{\partial x_j} + \frac{\partial \overline{U}_j}{\partial x_i} \right) - \frac{2}{3}k\delta_{ij} \qquad (4)$$

$$\nu_t = C \left| \overline{\overline{\omega}} \right|^\alpha k^{(1-\alpha)/2} \Delta^{(1+\alpha)} \qquad (5)$$

The filtered incompressible equations are solved by the in-house EllipSys3D code [14,15]. The code is based on a multiblock/cell-centered finite volume discretization of the steady/unsteady incompressible Navier–Stokes equations in primitive variables (pressure and velocity). The predictor–corrector method is used. In the predictor step, the momentum equations are discretized using a second-order backward-differentiation scheme in time and second-order central differences in space, except for the convective terms that are discretized by the QUICK upwind scheme. The obtained Poisson pressure equation is solved by a five-level multigrid technique. Because the EllipSys3D code is programmed using a multi-block topology, it can easily be parallelized using a message-passing interface.

3. Results and discussions

3.1 Flow configurations

The present numerical study is aimed at validations against previous wind tunnel measurements. Therefore, the airfoil geometry and flow conditions are set according to the experiments:

1. Airfoil: DTU-LN118 airfoil, chord=0.6m, span=1.8m (0.6m used for noise integration), serration length=16.7%-chord
2. Angles of attack: 0 degrees and 8 degrees. (geometrical angle in the wind tunnel)
3. Wind speed=45 m/s. Sound speed=344 m/s.
4. TE types: (a) original TE (without serration), (b) TE with serration: 16.7%-chord.

The airfoil under investigation is the in-house designed low noise airfoil with 18% relative thickness. Noise signal is collected along a span of 0.6m. As depicted in Figure 1, the integration region is marked with red square and it is located on the airfoil suction side. Similar procedure is carried out during LES simulation where Eq.(2) is applied in same region over the suction wall surface. LES simulations were conducted at a wind speed of 45m/s and angles of attack of 0 and 8 degrees. Flow over airfoils with and without serration is considered.
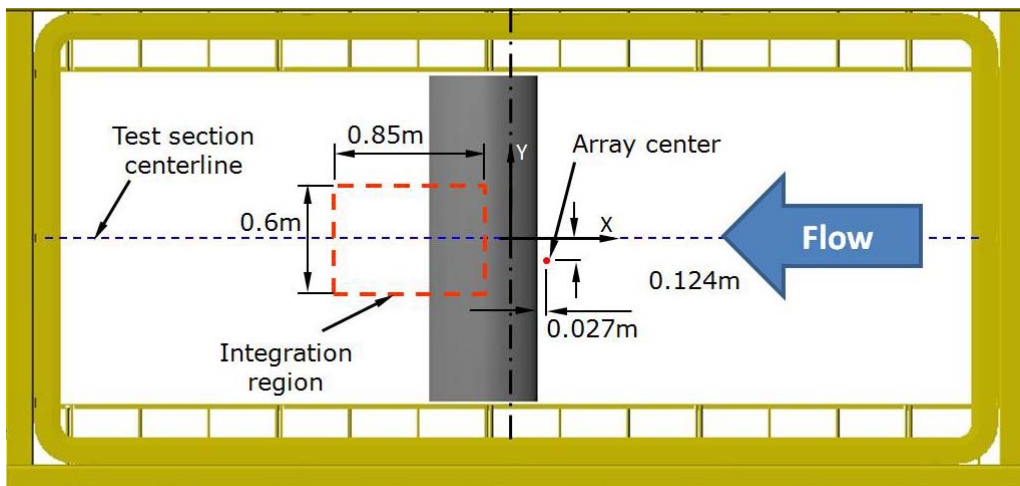

Figure 2. Test section of the Virginia Tech Stability Wind Tunnel.

As shown in Figure 3, a structured C-mesh is generated for turbulent flow simulation. According to the earlier works [16,17], the mesh resolution in terms of wall units shall be small and satisfy certain cell aspect ratio limitations. In the present case, the first wall cell size is in the order of 10^{-5} chords and the ratio of $\Delta x/\Delta y$ is around 25 along the airfoil wall surface. To study the influence of span-width, two meshes are created which include one serration and three serrations. Periodic flow condition is assumed at the two ends. Figure 3 shows the mesh configuration including three serrations. The total number of blocks is 140 and 420 for the meshes with one and three serrations, respectively. The flow solutions using one and three serrations are compared in the next section.
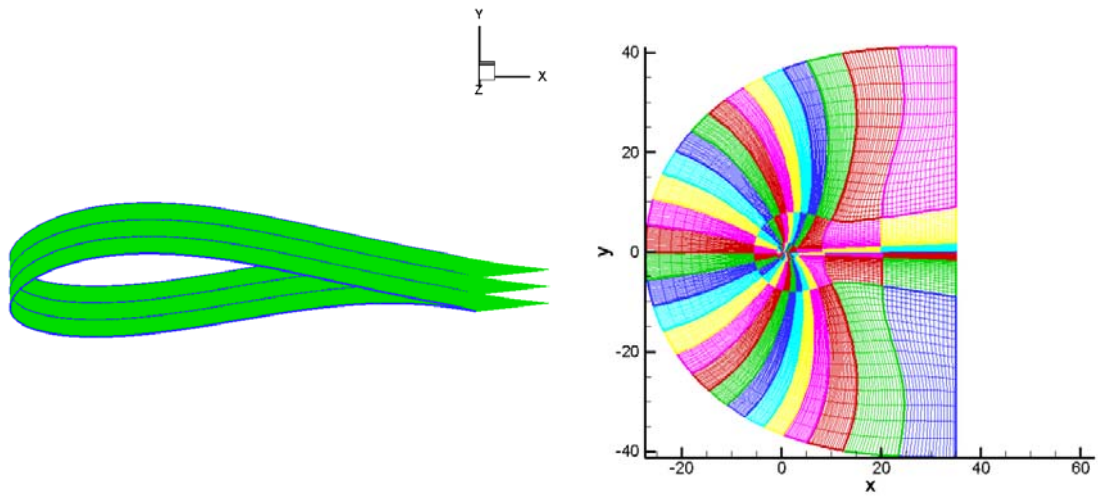
Figure 3. Mesh of the wall surfaces (left) and side view of mesh (right).

3.2 Comparisons

The root mean square (RMS) horizontal velocity contour and the streamlines are shown in Figure 4 at an angle of attack 6.07^{o} (8° geometrical angle). The contour slice is a cut across the tip of the serration where the flow over the serration area is depicted in the figure. At this angle of attack, it is seen that the flow is far from stall and still well-attached on the wall surface.
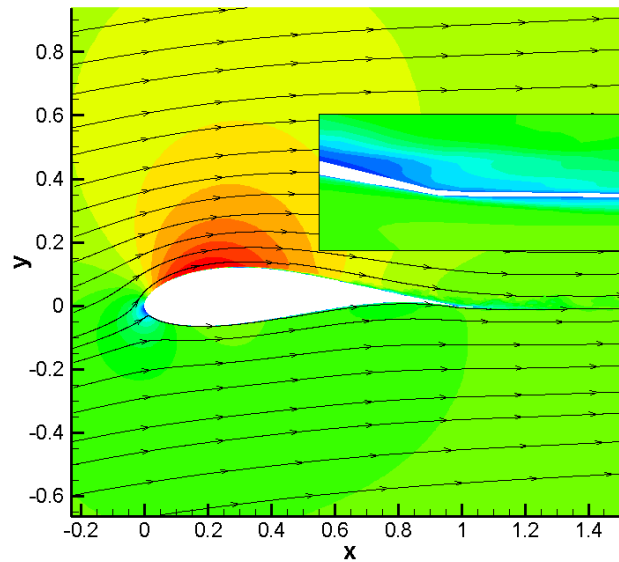

Figure 4. Contour of horizontal flow velocity and stream lines.

From the numerical simulations, no significant effect from the serration is found on the aerodynamic side. The pressure coefficients are compared for the original airfoil and the airfoil with serration. Again, the slice is cut through the tip of serration. Figure 5 shows the C_p values along the chord direction. At an angle of attack of -1.34^o (0° geometrical angle), general agreements are observed between measured data and the computations of none/serrated airfoils. It has to be mentioned that the experimental data for the none/serrated airfoils are very close. Therefore only one set of measured data is presented. Figure on the right hand side is the case for an angle of attack 6.07^o which shows same trend but with some better agreement. It is also expected that LES works better at a relative larger angle of attack where the size of turbulence eddies is relatively bigger.
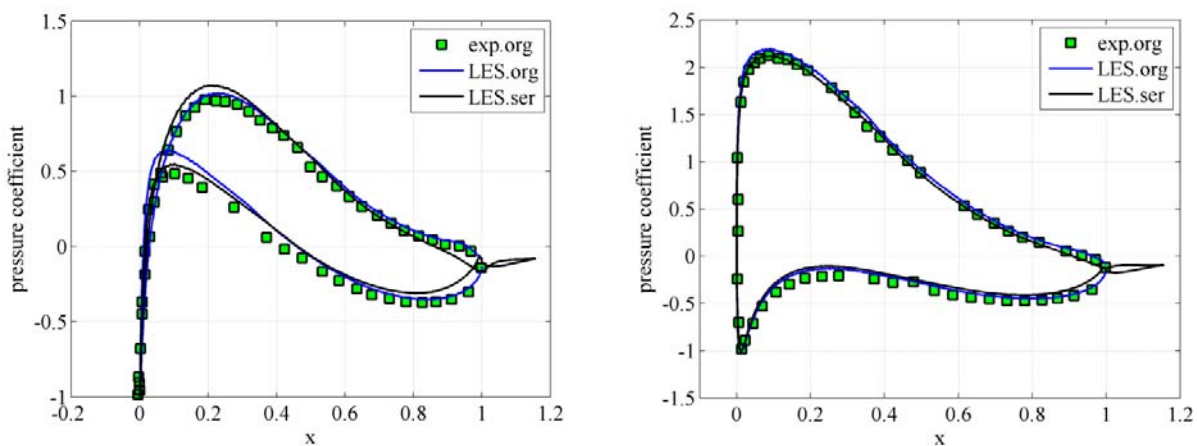

Figure 5. Cp compared at geometrical angle of attack 0° and 8°.

For the current LES simulations of TE serration, the computational efficiency has been considered as an important factor. It is expected that the use of a large span size with more serrations represents flow-field better than using a narrow span. It is often a practical issue of choosing resonable span size, which is typically limitted by the avialable computer resources. The left plot in Figure 6 shows the Cp results computed with *SpanA* and *SpanB* where *SpanA* contains 3 serrations and *SpanB* contains 1 serration. The difference between the two curves is hardly seen from the plot that indicates flow three-dimensionality is not playing an important role at this angle of attack. Some similar observation is found by Mary and Sagaut [16] where effects of using small span size is investigated. However, attention should be paid at very large angles of attack where three dimentional effect can be more significant. On the right plot in Figure 6, the Cp values are compared at two spanwise locations: the values cut through serration tip (*SliceA*) and through serration root (*SliceB*). As it can be seen that *SliceA* has an extended area at trailing edge which is due to the contribution from the serration. As observed from the comparion, some small deviation does exist near the traling edge, which only makes little change in flow-field but is enough to generate noise at different levels. A contour plot of wall pressure coefficient is also given in Figure 7 where no significant pressure variation exists along the airfoil span.
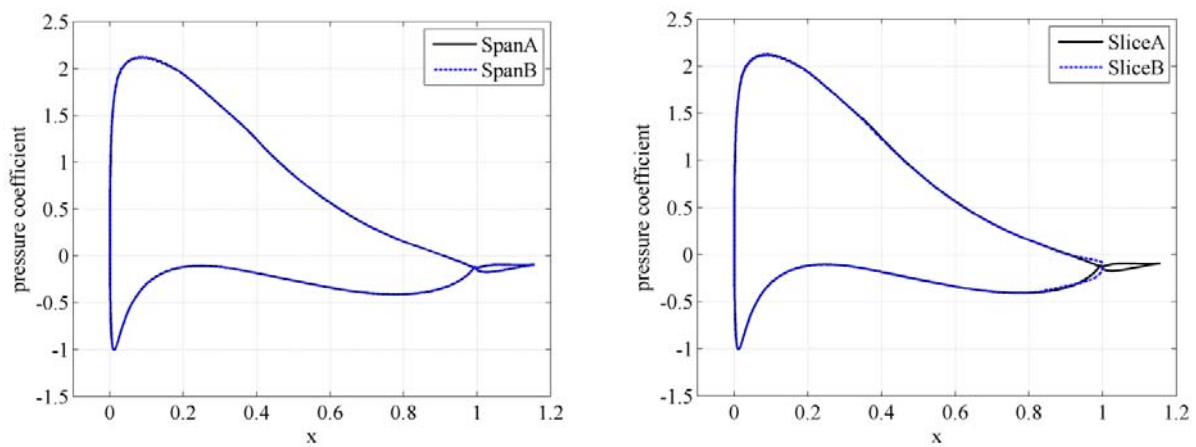
Figure 6. Cp comparisons with effect of different span size (left) and with a same span size but cut at different spanwise locations (right).
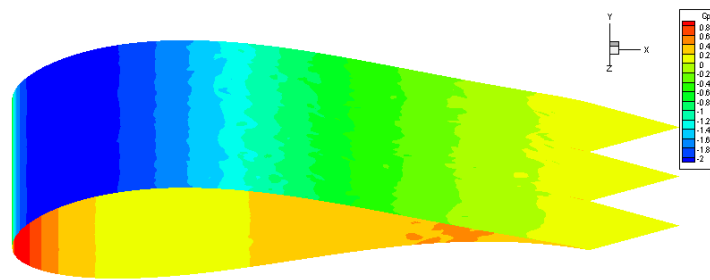

Figure 7. Normalized wall surface pressure.

Even though the aerodynamic field is so similar for the non/serrated airfoils, the generated sound field has larger deviations, see Figure 8 and Figure 9. For a stationary airfoil, the thickness term of the Farassat [13] formulation is not applied. Therefore, the integration of time derivative of aerodynamic pressure is the key parameter for noise prediction. For fair comparisons with experiments, Equation (2) is only applied at trailing edge part on the airfoil suction side. At the small angle of attack, the noise level is reduced in the higher frequency range, as shown in Figure 8. The experimental data shows no noise reduction at frequencies below 2 kHz. On the numerical side, larger noise reduction is seen in the high frequency range but some small reduction at low frequencies is also observed. In Figure 9, as the angle of attack is increased, the noise spectra are shifted towards low frequency as compared to Figure 8. As the suction side boundary layer thickness increases with angle of attack, the noise spectrum calculated on airfoil suction side shifts to low frequency range. On the contrary to the previous case, the noise reduction is only observed at frequencies below 2kHz. It seems that at larger angle of attack, the noise spectra are not affected by the serration at higher frequencies at all. As low frequency noise propagates for longer distance,

it makes sense to implement TE serrations at the outer part of blade where angle of attack is similar as the case shown in Figure 9. There are many other factors that might influence the efficiency of the serration, such as the serration length (root to tip length), wave length (width), flap angle (attached angle at TE), etc. It is expected that TE noise can be reduced for most kind of serration shapes before stall angle of attack.
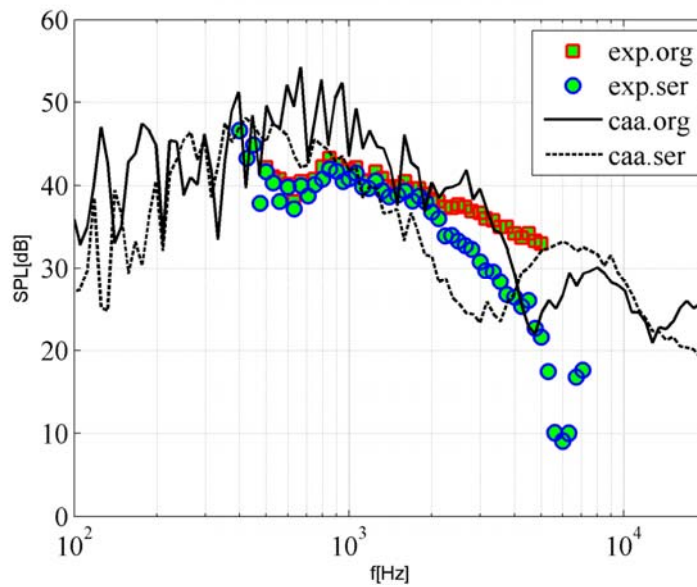

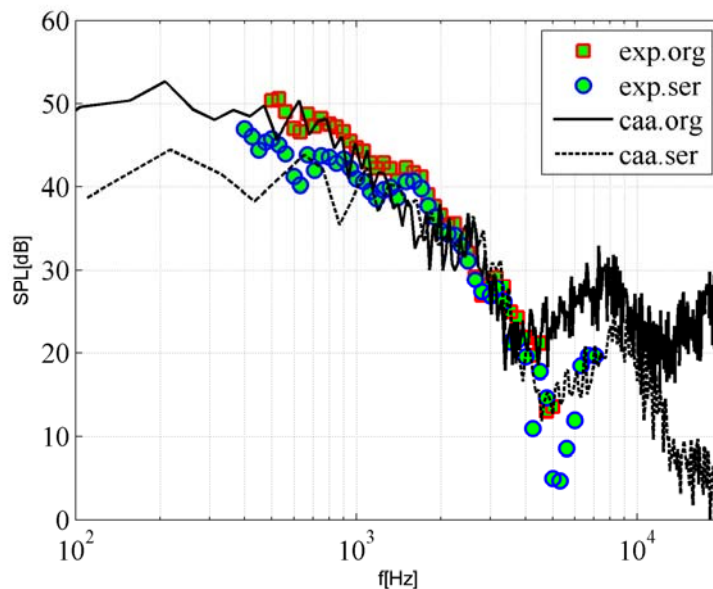Figure 8. Comparisons of simulated noise spectra against measurements at an angle of attack of 0°.

Figure 9. Comparisons of simulated noise spectra against measurements at an angle of attack of 8°.

4. Conclusions

In the current work, TE noise from a wind turbine airfoil is simulated with and without TE serration. As the first step, LES simulations are carried out to obtain a converged turbulence flow-field. At the next step, acoustic computations using the acoustic analogy is performed together with LES. It is observed that the general flow-field is weakly affected by the serration. The major difference is found from the wall pressure curve at TE where the serration is located. Noise signal received at far-field is calculated by integrating the time dependent pressure source on the wall surface. It has been numerically shown that airfoil trailing edge noise can be reduced by adding the serration. The acoustic results are obtained at 0 ang 8 degrees geometrical angle. Relative good agreements are found as compared with measured acoustic spectra. The noise generated at TE is reduced at high frequencies for low angle of attack, and is reduced at low frequencies for higher angle of attack.

References

[1] Wolf A, Lutz T, Würz W, Krämer E, Stalnov O, Seifert A (2014) *Trailing edge noise reduction of wind turbine blades by active flow control* Journal of Wind Energy, online: 17 MAR 2014, DOI: 10.1002/we.1737.

[2] Hutcheson F V (2005) *PIV measurements on a blowing flap* NASA report AIAA 2005-212.

[3] Herr M, Dobrzynski W (2005) *Experimental investigations in low-noise trailing-edge design* AIAA J. 43(6), 1167-1175.

[4] Finez A, Jondeau E, Roger M, Jacob MC (2010) *Brodband noise reduction with trailing edge brushes* AIAA paper 2010-3980.

[5] Howe MS (1978) *A review of the theory of trailing edge noise* J. Sound Vib., 61(3), 437-465.

[6] Howe MS (1991) *Noise produced by a sawtooth trailing edge* Journal of the Acoustic Society of America, 90(1), 482–487

[7] Braun KA, van der Borg NJCM, Dassen AGM, Doorenspleet F, Gordner A, Ocker J, Parchen R (1999) *Serrated trailing edge noise* EU Wind Energy Conference.

[8] Chong TP, Joseph PF (2013) *An experimental study of airfoil instability tonal noise with trailing edge serrations* J. Sound Vib., 332(24): 6335-6358, 2013.

[9] Oerlemans S, Fisher M, Maeder T, Kögler K (2009) *Reduction of wind turbine noise using optimized airfoils and trailing edge serrations* AIAA J. 47(6), 1470-1481.

[10] Gruber M , Joseph P and Chong T(2010) *Experimental investigation of airfoil self-noise and turbulent wake reduction by the use of trailing edge serrations* 16th AIAA/CEAS Aeroacoustics Conference, Stockholm

[11] Sandberg RD and Jones LE (2011) *Direct numerical simulations of low Reynolds number flow over airfoils with trailing-edge serrations* Journal of Sound and Vibration, Vol 330(16), 3818-3831, doi:10.1016/j.jsv.2011.02.005

[12] Ffowcs Williams JE and Hawkings DL(1969) *Sound Generated by Turbulence and Surfaces in Arbitrary Motion* Philosophical Transactions of the Royal Society, Vol. A264, pp. 321-342.

[13] Farassat F (2007) *Derivation of formulations 1 and 1A of Farassat* NASA/TM-2007-214853.

[14] Michelsen JA (1998) *General Curvilinear Transformation of the Navier-Stokes Equations in a 3D Polar Rotating Frame* Technical Report AFM 1998-01; Technical University of Denmark.

[15] Sørensen, NN (1995) *General Purpose Flow Solver Applied Over Hills* RISØ-R-827-(EN) 1995; Risø National Laboratory, Denmark.

[16] Mary I and Sagaut P (2002) *Large eddy simulation of flow around an airfoil near stall* AIAA J. Vol. 40, No. 6

[17] Zhu WJ, Shen WZ, Bertagnolio F and Sørensen JN (2012) *Comparisons between LES and wind tunnel hot-wire measurements of a NACA 0015 airfoil* Proceedings of EWEA 2012 - European Wind Energy Conference & Exhibition. European Wind Energy Association (EWEA), 975-982